Structural properties and thermal conductivity of crystalline Ge clathrates

G. S. Nolas
R & D Division, Marlow Industries, Incorporated, 10451 Vista Park Road, Dallas, Texas 75238

T. J. R. Weakley
Department of Chemistry, University of Oregon, Eugene, Oregon 97403

J. L. Cohn
Department of Physics, University of Miami, Coral Gables, Florida 33124

R. Sharma
Center for Solid State Science, Arizona State University, Tempe, Arizona 85287
(Received 14 May 1999; revised manuscript received 12 October 1999)

Structural analysis and thermal conductivity data on $Sr_8Ga_{16}Ge_{30}$ and $Eu_8Ga_{16}Ge_{30}$ crystals are reported. These compounds form in the cubic space group $Pm\bar{3}n$ with lattice parameters of 10.721(2) and 10.703(2) Å respectively. Single-crystal x-ray diffraction and structural refinement indicate that the randomly distributed Ga and Ge atoms form a tetrahedrally bonded three-dimensional net in whose cavities the ''guest'' Sr or Eu atoms reside. The ''guest'' atoms in the smaller of these polyhedra (dodecahedra) have spherical thermal ellipsoids while those in the larger polyhedra (tetrakaidecahedra) display relatively large and highly anisotropic thermal ellipsoids. The low-thermal conductivity of these compounds at low temperatures is attributable to the disorder introduced by the dynamic ''rattling'' introduced by these ''guest'' atoms inside the polyhedra. The potential of this material system for thermoelectric applications is also discussed.

INTRODUCTION

There is now growing interest in ''open structured'' (zeolitelike) semiconducting compounds for thermoelectric applications due to their characteristically low-thermal conductivities. The host atoms in such materials form weak bonds with interstitial atoms occupying ''voids'' in these structures, thus resulting in localized vibrational modes. These localized modes resonantly scatter acoustic-mode, heat-carrying phonons. This phenomena is well documented in the skutterudite material system where very low-thermal conductivities were observed upon filling the voids with lanthanide ions.[1] The smaller and more massive the lanthanide ion the lower thermal conductivity. Recent inelastic neutron scattering data support this picture.[2]

In light of the demonstration that the phonon-glass, electron crystal approach[3] is of importance in materials research for thermoelectric applications, other ''open structured'' systems are also presently under investigation. Of particular recent interest are compounds that form the clathrate hydrate crystal lattice structure.[4–6] One such compound, $Sr_8Ga_{16}Ge_{30}$, forms in the type-I clathrate structure analogous to the gas clathrate hydrate $(Cl_2)_8(H_2O)_{46}$. Very low temperature (<1 K) thermal conductivity κ measurements on polycrystals indicate a T^2-temperature dependence, similar to that found in amorphous materials, while higher temperature data indicate a minimum in the 10–30 K range, attributable to resonance scattering.[4,5] At room temperature $\kappa \sim 1$ W/mK for $Sr_8Ga_{16}Ge_{30}$. Along with relatively high-electrical conductivity and Seebeck coefficients[4–6] these results demonstrate the potential of these materials for thermoelectric applications. In this paper, we report on single-crystal structural and low temperature κ measurements on two Ge clathrates, $Sr_8Ga_{16}Ge_{30}$ and $Eu_8Ga_{16}Ge_{30}$, with the aim of investigating the correlation between the crystal structure and the low, glasslike κ values observed for these compounds.

SAMPLE PREPARATION AND THERMAL CONDUCTIVITY RESULTS

The Ge-clathrate crystals were similarly prepared, as follows. Stoichiometric quantities of high purity constituent elements were mixed and reacted in pyrolitic boron nitride (BN) crucibles for three days at 950 C then annealed at 700 C for four days. The BN crucibles were themselves sealed inside a fused quartz ampule, which was evacuated and backfilled with argon gas to a pressure of two-thirds of an atmosphere. The ingots were composed of crystallites with dimensions of one to three cubic millimeters. The ingots were stable in air and water but were etched with aqua regia for metallographic analysis. Extensive electron-beam microprobe analysis on polished surfaces of each sample revealed the exact composition of these crystals and demonstrated the homogeneity throughout each ingot.

Specimens for transport measurements were cut to dimension $4\times1\times1$ mm^3 by a wire saw using 50 micron tungsten wire to ensure damage free samples. Four-probe electrical resistivity (ρ) and steady-state thermal conductivity (κ) were measured in a radiation-shielded vacuum probe with the heat flow measured along the longest axis. Heat losses via conduction through the lead wires and radiation were determined in separate experiments and the data corrected accordingly. These corrections were 10–15 % at room temperature

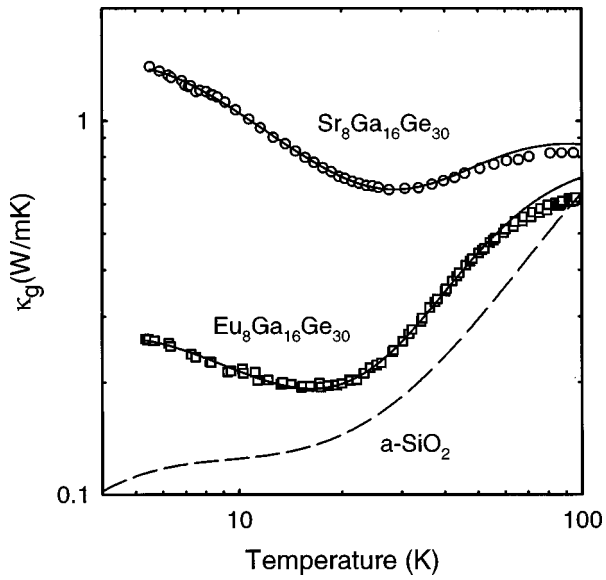

FIG. 1. Thermal conductivity vs temperature for crystalline $Sr_8Ga_{16}Ge_{30}$ (open circles), $Eu_8Ga_{16}Ge_{30}$ (open squares) and amorphous Ge (dashed line). Solid lines are fits to the phenomenological model described by Eq. (3) and discussed in the text. The fitting parameters for the Sr(Eu) filled specimens were $A=9.0\times10^3$ (4.2×10^4) $m^{-1}K^{-1}$, $B=20\times10^{-3}$ (35×10^{-3}) K^{-2}, $C_1=1.80\times10^{-31}(2.83\times10^{-31})$ $m^{-1}K^{-2}s^{-2}$, $C_2=2.91\times10^{-31}\times(4.91\times10^{-31})$ $m^{-1}K^{-2}s^{-2}$, $D=0.6$ (2.0) $m^{-1}K^{-1}$, $\gamma_1=0.8$ (0.8), $\gamma_2=1.7$ (1.8), and $l_{min}=3.0$ (4.5) Å.

and less than 2% below 120 K.

Figure 1 shows the lattice component of κ, κ_g, for the two crystalline Ge clathrates computed by subtracting from κ the Wiedemann-Franz law estimate of the electronic contribution, $\kappa_e=L_0T/\rho$ ($L_0=2.44\times10^{-8}$ $W\Omega/K^2$), in the range $5<T<100$ K. Also shown in Fig. 1 is κ of vitreous silica (a-SiO_2).[7] The solid line fits to the data will be described in detail in the next section. We note κ_g for the Ge clathrates are more than one order of magnitude lower than that for crystalline Ge (not shown in the figure) and similar in magnitude to a-SiO_2. There is also an obvious ''resonance dip'' in the $Sr_8Ga_{16}Ge_{30}$ sample in the 20 to 40 K. $Eu_8Ga_{16}Ge_{30}$ has lower κ_g at all temperatures and a more pronounced ''dip.'' As suggested previously,[4,5] we anticipate that the Eu^{2+} ion will have a larger effect on κ_g than will Sr^{2+} since Eu^{2+} is more massive. A similar resonance scattering of phonons is likely the principle mechanism determining low κ_g values in the lanthanide-filled skutterudites[1] and clathrate hydrates.[3]

CRYSTAL STRUCTURE ANALYSIS AND DISCUSSION

Very small single crystals were isolated and investigated employing an Enraf-Nonius CAD-4 single-crystal diffractometer with graphite monochrometer and Mo $K\alpha$ radiation. The Laue symmetry $m3m$ was confirmed by the measurement of potential equivalents for several reflections. The structural refinement confirmed the assignment of space-group $Pm\bar{3}n$ (no. 223) for these compounds corresponding to the type-I clathrate structure. Absorption corrections based on azimuthal scans were applied. No attempt was made to distinguish between Ga and Ge although neutron scattering data indicate these to be randomly distributed.[8] The TEXSAN program suite[9] incorporating complex atomic scattering factors, was used in all calculations.

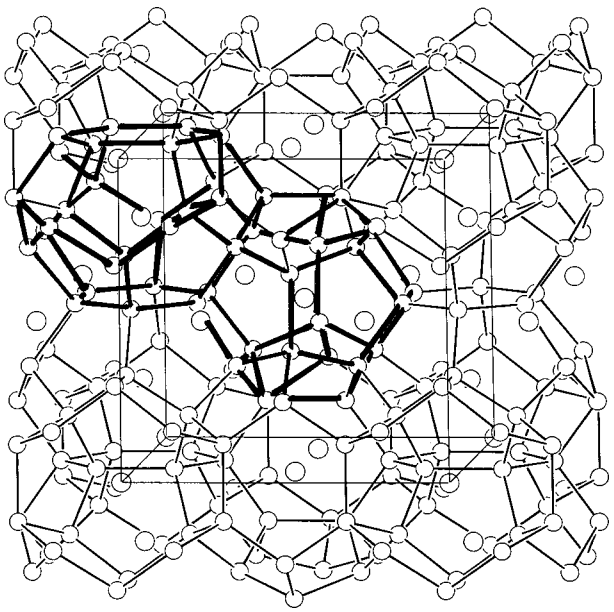

FIG. 2. The type-I clathrate crystal structure. Outlined are the two different polyhedra that form the unit cell with the dodecahedron in the center and the tetrakeidecahedron to the left.

Figure 2 is a schematic illustrating the type-I clathrate crystal structure. The (Ga, Ge) framework atoms form bonds in a distorted tetrahedral arrangement. They form polyhedra that are covalently bonded to each other by shared faces. There are eight polyhedra per cubic unit cell, Ge_{20} dodecahedra and Ge_{24} tetrakaidecahedra in a 1:3 ratio. These two polyhedra are outlined in Fig. 2. The Sr and Eu atoms reside inside these polyhedra, at the $2a$ and $6b$ crystallographic positions, respectively.

From our single-crystal x-ray diffraction analysis the Ge-Ge-Ge bond angles range from 106° to 125°, implying bonding that is similar to the sp^3 hybridization in diamond-structured germanium. The Ge-Ge bond lengths in $Sr_8Ga_{16}Ge_{30}$ and $Eu_8Ga_{16}Ge_{30}$ are slightly larger than that of diamond-structured germanium at 2.4498 Å. Employing the results from our structural refinements we can estimate the average radii of the Ge_{20} and Ge_{24} polyhedra, assuming the shortest interatomic distances. These are, respectively, 2.197 and 2.377 Å for $Sr_8Ga_{16}Ge_{30}$, and 2.183 and 2.365 Å for $Eu_8Ga_{16}Ge_{30}$. The sizes of these polyhedra are similar to those found for other type-I Ge clathrates.[10–13] This seems to indicate that the cage size is a function of the framework atoms and not the ''guest'' atoms. This is quite interesting since it suggests that appropriate ''guest'' atoms incorporated into the polyhedra might further reducing κ towards κ_{min},[14] the theoretical minimum thermal conductivity. The positions and thermal ellipsoids are given in Tables I and II. Note the Ge(1), Ge(2), and Ge(3) sites also apply to the Ga atoms; the Ga and Ge distribution in the structure is assumed random.

Small crystal fragments of the two compounds were crushed into a fine powder using agate mortar and pestle for transmission electron microscopy (TEM) analysis. A drop of a suspension of the powder in 99.9% ethanol was dispersed

TABLE I. Atomic parameters for $Sr_8Ga_{16}Ge_{30}$ in space group $Pm\bar{3}n$ with a lattice parameter of 10.721(2), one formula unit (54 atoms) per cubic unit cell and a calculated density of 5.381 g/cm^3. The anisotropic thermal parameters are defined by $T=\exp(-2\pi^2\Sigma_i\Sigma_j U_{ij}h_ih_ja_i^*a_j^*)$. The equivalent isotropic thermal parameter is defined by $B_{eq}=(8\pi^2/3)\Sigma_i\Sigma_j U_{ij}a_i^*a_j^*a_ia_j)$.

Atom	Sr(1)	Sr(2)	Ge(1)	Ge(2)	Ge(3)
site	2*a*	6*d*	6*c*	16*i*	24*k*
x	0.0000	0.2500	0.2500	0.18416(8)	0.0000
y	0.0000	0.5000	0.0000	0.1842	0.30888(11)
z	0.0000	0.0000	0.5000	0.1842	0.11714(12)
U_{11} (Å^2)	0.0159(9)	0.02325(21)	0.0116(13)	0.0104(3)	0.0118(6)
U_{22} (Å^2)	0.0159	0.1126(29)	0.0125(8)	0.0104	0.0094(6)
U_{33} (Å^2)	0.0159	0.1126	0.0125	0.0104	0.0107(6)
U_{12} (Å^2)	0.0000	0.0000	0.0000	−0.007(3)	0.0000
U_{13} (Å^2)	0.0000	0.0000	0.0000	−0.0007	0.0000
U_{23} (Å^2)	0.0000	0.0000	0.0000	−0.0007	−0.0017(6)
B_{eq} (Å^2)	1.258(12)	6.54(7)	0.96(3)	0.818(4)	0.84(2)

in a holey carbon film on copper grids. A JEOL 4000EX TEM microscope with a double-tilt lift top entry holder operated at 400 KV was used for selected area electron diffraction (SAED) and high-resolution electron microscopy (HREM) imaging. Thin crystal fragments were aligned along one of the low-index zones and both SAED patterns and HREM images were recorded on photographic films. These results are shown in Fig. 3 for $Sr_8Ga_{16}Ge_{30}$.

Figure 3(a) shows a HREM image oriented along the ⟨111⟩ zone axis. The dark spots correspond to atom positions. The bright spots, hexagonal faces, reveal the ''tunnels'' formed by the chain of tetrakaidecahedra (Ge_{24}) along the ⟨111⟩ direction. Also inset in Fig. 3(a), at the upper left hand corner, is a calculated image for a crystal thickness of 70.6 and −400 Å (near Scherzer defocus) while in the middle of this figure a structure model in this orientation is inset. Figure 3(b) is an SAED image in the ⟨111⟩ orientation. Again a hexagonal pattern is clearly observed. Similar images were observed for $Eu_8Ga_{16}Ge_{30}$. The lattice parameters from this analysis were in agreement with the single crystal x-ray data.

The specific framework and thermal parameters, or atomic displacement parameters (ADP's), are important aspects of this structure. Particularly interesting are the anisotropic ADP's (U_{ij}) for the $X(2)$ ''guest'' atoms, where X = Sr or Eu. This is illustrated in Fig. 4 for the $Eu_8Ga_{16}Ge_{30}$ sample and tabulated in Table II. Although Fig. 4 indicates data for the $Eu_8Ga_{16}Ge_{30}$ sample, that for $Sr_8Ga_{16}Ge_{30}$ is similar however with smaller amplitude ADP's. Note the difference in the ADP's between the $X(2)$ atoms and the $X(1)$ atoms in each compound. The $X(1)$ atoms have symmetric ADP's that are slightly larger in magnitude to that of the (Ga, Ge) framework atoms. The $X(2)$ atoms exhibit ADP's that are almost an order of magnitude larger than those of the other constituent atoms. Large and anisotropic ADP's are typical of compounds with this type of crystal structure. The large ADP's for the $X(2)$ atoms indicate the possibility of a static disorder in addition to the dynamic, or ''rattling'' motion. The electrostatic potential within the polyhedra are not everywhere the same and different points may be energetically preferred. This would suggest that the $X(2)$ atom can then tunnel among the different energetically preferred posi-

TABLE II. Atomic parameters for $Eu_8Ga_{16}Ge_{30}$ in space group $Pm\bar{3}n$ with a lattice parameter of 10.703(2), one formula unit (54 atoms) per cubic unit cell and a calculated density of 6.106 g/cm^3. The anisotropic thermal parameters are defined by $T=\exp(-2\pi^2\Sigma_i\Sigma_j U_{ij}h_ih_ja_i^*a_j^*)$. The equivalent isotropic thermal parameter is defined by $B_{eq}=(8\pi^2/3)\Sigma_i\Sigma_j U_{ij}a_i^*a_j^*a_ia_j)$.

Atom	Eu(1)	Eu(2)	Ge(1)	Ge(2)	Ge(3)
site	2*a*	6*d*	6*c*	16*i*	24*k*
x	0.0000	0.2500	0.2500	0.18386(12)	0.0000
y	0.0000	0.5000	0.0000	0.1839	0.30914(19)
z	0.0000	0.0000	0.5000	0.01839	0.11677(18)
U_{11} (Å^2)	0.0149(8)	0.0226(20)	0.0132(20)	0.0086(4)	0.0093(8)
U_{22} (Å^2)	0.0149	0.181(5)	0.0097(12)	0.0086	0.0093(9)
U_{33} (Å^2)	0.0149	0.1807	0.0097	0.0086	0.0080(8)
U_{12} (Å^2)	0.0000	0.0000	0.0000	−0.0011(5)	0.0000
U_{13} (Å^2)	0.0000	0.0000	0.0000	−0.0011	0.0000
U_{23} (Å^2)	0.0000	0.0000	0.0000	−0.0011	−0.0009(9)
B_{eq} (Å^2)	1.174(10)	10.11(9)	0.86(4)	0.682(6)	0.70(2)

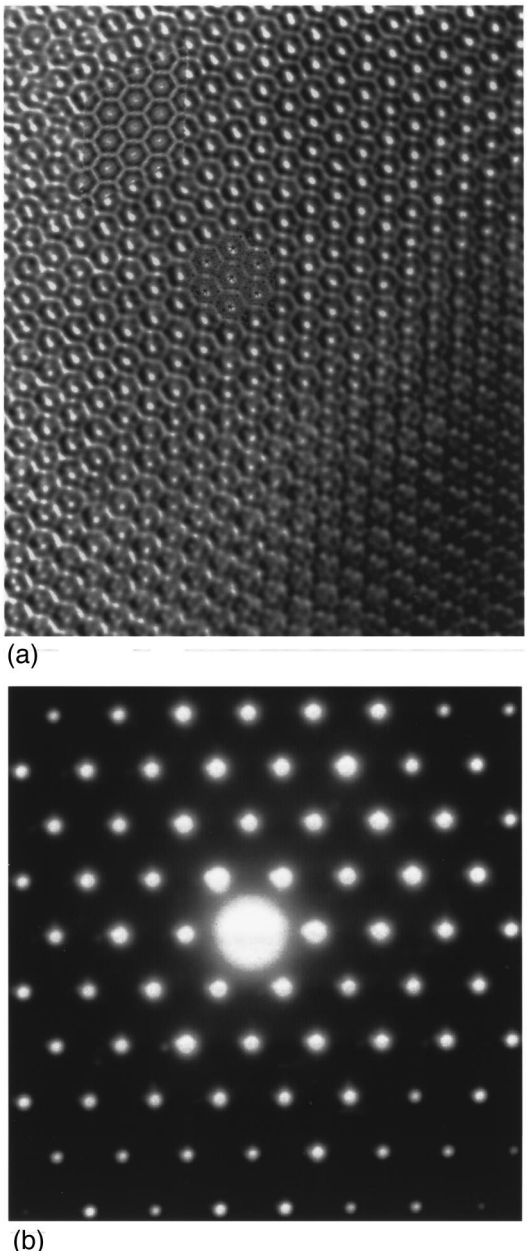

FIG. 3. HREM image (a) and SAED pattern (b) of a crystal fragment oriented with ⟨111⟩ zone axis parallel to the electron beam.

tions. The possibility of a ''freeze-out'' of the ''rattling'' motion of Sr^{2+} in $Sr_8Ga_{16}Ge_{30}$ was indicated in our low-temperature κ_g data on polycrystals.[4] This data was successfully fit to a tunnel-states model normally employed to explain low temperature data of amorphous materials. The implication is that static disorder is associated with a spatial distribution of the $X(2)$ ion positions inside the polyhedra. It is plausible that the large measured ADP's contain both a static as well as a dynamic component. We may therefore reevaluate the structural data in order to include such a possibility and compare these results to thermal conductivity data. We rely on recent temperature-dependent ADP's for $Sr_8Ga_{16}Ge_{30}$ from refinements of neutron diffraction data[8] in modeling our room-temperature data in order to give the most physically reasonable results.

Table III shows the atomic parameters with structural refinements such that the $X(2)$ site is no longer centered in a D_{2d} crystallographic point symmetry but is disordered in four equivalent off-center positions, approximately 0.36 and 0.45 Å away from the center position $(1/4,1/2,0)$ for Sr(2) and Eu(2), respectively. The average crystal symmetry however remains $Pm\bar{3}n$. Figure 5 illustrates the case for $Eu_8Ga_{16}Ge_{30}$. An attempt to distinguish between the dynamic and static disorder is apparent from this figure. By imposing the fractional occupation of the $X(2)$ site, the ADP's are smaller but still much larger than that of the other constituents. This is essentially an attempt to remove much of the static, or positional, disorder from the ADP data. Clearly, both static and dynamic disorder play a role in the $X(2)$ atom positions in the crystal lattice. Both mechanisms have an effect on κ_g. We note that this fractional occupation of the $X(2)$ site does not change the structural refinement very much. In addition, good refinement can also be achieved assuming anisotropic ADP's. These data can be obtained from the authors upon request.

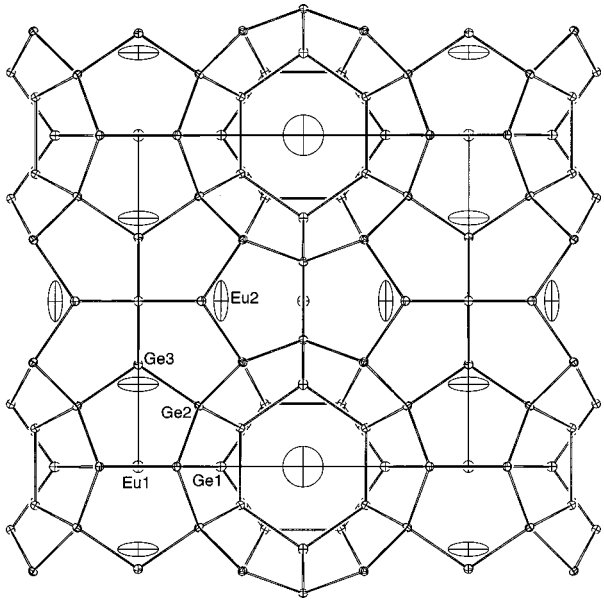

FIG. 4. Crystal structure projection on a (100) plane of $Eu_8Ga_{16}Ge_{30}$ illustrating the large anisotropic atomic displacement parameters.

Recently,[15] it has been shown that ADP's can be used to determine characteristic localized vibration frequencies for weakly bound atoms that ''rattle'' within their atomic ''cages.'' This approach, which assumes the ''rattling'' atoms act as harmonic oscillators, has been successfully applied to the case of skutterudite compounds.[15] The localized vibration of the ''rattler'' atom can be described by an Einstein oscillator model such that $U=k_BT/m(2\pi\nu)^2$ where U is the isotropic mean-square displacement, k_B is Boltzmann's constant, m is the mass of the ''rattling'' atoms under the assumption their ''cages'' are relatively rigid and ν the frequency of vibration. The ADP data can then be used to estimate the ''Einstein temperature'' of these atoms, $T_E=h\nu/k_B$, where h is Planck's constant. Employing this approach we obtain $T_E=74$ and 103 K for Sr(2) and Sr(1), respectively, for $Sr_8Ga_{16}Ge_{30}$ and $T_E=53$ and 82 K for Eu(2) and Eu(1), respectively, for $Eu_8Ga_{16}Ge_{30}$.

It is instructive to employ this partial-occupation model in

TABLE III. Atomic parameters for $Sr_8Ga_{16}Ge_{30}$ (top data) and $Eu_8Ga_{16}Ge_{30}$ (bottom data) modeled with $X(2)$ (where X=Sr or Eu) in four equivalent positions within the {100} planes about the center point (1/4,1/2,0). The $X(2)$ site is therefore 25% occupied. The equivalent isotropic thermal parameter is defined by $B_{eq}=(8\pi^2/3)\Sigma_i\Sigma_j U_{ij}a_i^*a_j^*a_ia_j$).

Atom site	$X(1)$ 2a	$X(2)$ 24k	Ge(1) 6c	Ge(2) 16i	Ge(3) 24k
x	0.0000	0.2524(11)	0.2500	0.18418(7)	0.0000
	0.0000	0.2530(7)	0.2500	0.18389(8)	0.0000
y	0.0000	0.4667(5)	0.0000	0.18418	0.30888(11)
	0.0000	0.4577(4)	0.0000	0.18399(8)	0.30912(13)
z	0.0000	0.0000	0.5000	0.18418	0.11713(11)
	0.0000	0.0000	0.5000	0.18389(8)	0.11673(13)
B_{eq} (Å^2)	1.225(11)	2.34(14)	0.91(3)	0.803(4)	0.86(2)
	1.112(9)	2.69(11)	0.73(3)	0.651(5)	0.75(3)

evaluating our κ_g data of these two compounds. We first note that mass fluctuation scattering or grain boundary scattering cannot explain the temperature dependence of κ_g of these compounds. A model that incorporates the dynamic as well as static disorder associated with the encapsulated atoms is required. In our previous study[4] of κ_g in polycrystals of these compounds, we employed a phenomenological model for κ_g with a phonon mean-free path that is a sum of terms representing tunnel system (TS), resonant, and Rayleigh (R) scattering,[4]

$$\kappa=\frac{1}{3}\int_0^{\omega_D}\nu C(\omega,T)l(\omega)d\omega \tag{1}$$

$$l(\omega)=(l_{\rm TS}^{-1}+l_{\rm res}^{-1}+l_{\rm R}^{-1})^{-1}+l_{\rm min} \tag{2}$$

$$l_{\rm TS}^{-1}=A(\hbar\omega/k_B)\tanh(\hbar\omega/2k_BT)+(A/2)(k_B/\hbar\omega+B^{-1}T^{-3})^{-1} \tag{3}$$

$$l_{\rm res}^{-1}=\sum C_i\omega^2T^2/[(\omega_i^2-\omega^2)^2+\gamma_i\omega_i^2\omega^2] \tag{4}$$

$$l_{\rm R}^{-1}=D(\hbar\omega/k)^4, \tag{5}$$

where ω_D is the Debye frequency, C is the heat capacity of the phonons, v is the average sound velocity, ω is the frequency, T the absolute temperature, $\hbar$ is Planck's constant divided by 2π and γ is an average deformation potential. The lower limit on l is assumed to be a constant $l_{\rm min}$. The constants A and B in Eq. (3) are related to microscopic variables describing the TS model.[16] Their ratio is given by $A/B=n(\hbar v)^2/\pi k_B$, with n the density of tunnel states per volume strongly coupled to phonons. The TS scattering was introduced in Ref. 4 to model the glasslike $\kappa_g\propto T^2$ behavior observed in polycrystals for $T<1$ K. Though the present data for crystals are restricted to $T>5$ K, we retain this scattering contribution because it influences the computed κ_g up to $T=20$ K, and allows for a comparison of the present fit parameters with those determined previously for the polycrystals.

The most important difference between the present analysis and that of Ref. 4 is that we constrain the resonance frequencies to be equal to the two ''Einstein temperatures'' obtained from the structural data, with ω_1 and ω_2 corresponding to vibrations of the $X(1)$ and $X(2)$ guests, respectively. Excellent fits (solid curves in Fig. 1) are found using[8] $\Theta_D=270$ K and $v=2600$ m/s. The values for the fit parameters are listed in the caption of Fig. 1. Allowing a greater resonance width for the scattering by $X(2)$ vibrations improved the fits; the same γ_1 were used for both compounds to limit the parameter variations. The ratio of the resonance strengths should reflect the relative populations of the two vibrational modes and their relative scattering strengths. The fit results yield $C_1/C_2\approx1.7$ for both compounds; close to the value of 3 for the relative population of large cages to small cages. The values of A/B and D are a factor of 3 larger for the Eu compound than for the Sr compound, suggesting that the former is characterized by a larger density of strongly coupled tunnel systems (n) and greater mass density variations. It is plausible to attribute the TS with the (static) positional disorder of the guest atoms within the four, nominally equivalent $X(2)$ sites within the large cages. More

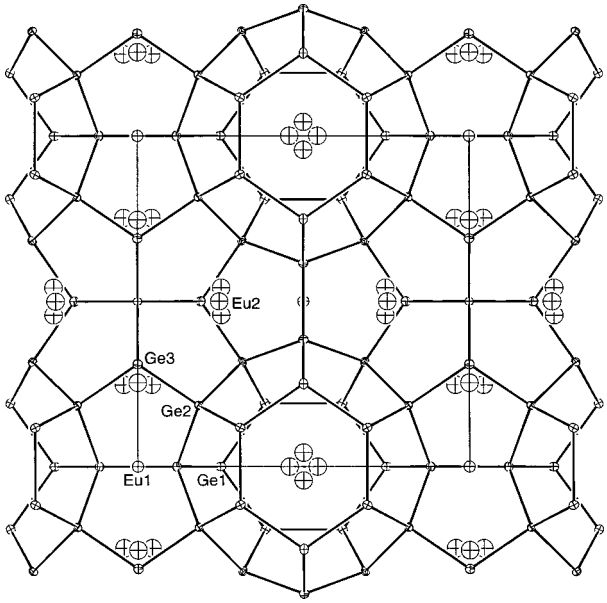

FIG. 5. The static and dynamic disorder of the Eu(2) site in $Eu_8Ga_{16}Ge_{30}$ is illustrated on a (100) plane for the case of isotropic atomic displacement parameters.

definitive conclusions about the resonances and their interactions with long-wavelength phonons might be afforded by spectroscopic studies of the guest vibrations.

CONCLUSION

We have attempted to correlate the thermal conductivity with the crystal structural of two crystalline Ge clathrates. Very large anisotropic ADP's of the Sr^{2+} and Eu^{2+} ions in the tetrakaidecahedra imply a large positional, or static, disorder in addition to the dynamic disorder associated with the ''rattling'' motion of these ions. The disorder induced by these ions has an enormous effect on the thermal transport of these compounds and is the reason for the observed ''glass-like'' temperature dependence in the thermal conductivity.

ACKNOWLEDGMENTS

It is a pleasure to acknowledge B. C. Chakoumakos and B. C. Sales of the Solid State Division at Oak Ridge National Laboratory and D. C. Johnson of the Chemistry Department at the University of Oregon for useful discussions. One of the authors (G.S.N.) gratefully acknowledges support from the Army Research Laboratory, Contract No. DAAD 17-99-C-006.

[1] G. S. Nolas, D. T. Morelli, and T. M. Tritt, Annu. Rev. Mater. Sci. **29**, 89 (1999), and references therein.

[2] V. Keppens, D. Mandrus, B. C. Sales, B. C. Chakoumakos, P. Dai, R. Coldea, M. B. Maple, D. A. Gajewski, E. J. Freeman, and S. Bennington, Nature (London) **395**, 876 (1998).

[3] G. A. Slack, in *CRC Handbook of Thermoelectrics*, edited by D. M. Rowe (CRC, Boca Raton, FL, 1994), p. 407, and references therein.

[4] G. S. Nolas, J. L. Cohn, G. A. Slack, and S. B. Schujman, Appl. Phys. Lett. **73**, 178 (1998).

[5] J. L. Cohn, G. S. Nolas, V. Fessatidis, T. H. Metcalf, and G. A. Slack, Phys. Rev. Lett. **82**, 779 (1999).

[6] G. S. Nolas, in *Thermoelectric Materials—The Next Generation Materials for Small-Scale Refrigeration and Power Generation Applications*, edited by T. M. Tritt, G. Mahan, H. B. Lyon, Jr. and M. G. Kanatzidis, MRS Symposia Proceedings No. 545 (Materials Research Society, Pittsburgh, PA, 1999), p. 435.

[7] D. G. Cahill, H. E. Fischer, T. Klitsner, E. T. Swartz, and R. O. Pohl, J. Vac. Sci. Technol. A **7**, 1259 (1989).

[8] B. C. Chakoumakos, B. C. Sales, D. G. Mandrus, and G. S. Nolas, J. Alloys Compd. **296**, 80 (1999).

[9] TeXsan Software for Single-Crystal Structure Analysis, version 1.7 (Molecular Structures Corporation, The Woodlands, TX, 1977).

[10] B. Eisenmann, H. Schafer, and R. J. Zagler, J. Less-Common Met. **118**, 43 (1986).

[11] W. Westerhaus and H. Z. Schuster, Z. Naturforsch. A **32b**, 1365 (1977).

[12] A. Czybulka, B. Kuhl, and H.-U. Schuster, Z. Anorg. Allg. Chem. **594**, 23 (1991).

[13] B. Kuhl, A. Czybulka, and H.-U. Schuster, Z. Anorg. Allg. Chem. **621**, 1 (1995).

[14] G. A. Slack, in *Solid State Physics*, edited by H. Ehrenreich, F. Seitz, and D. Trunbull (Academic, New York, 1979), Vol. 34, p. 1.

[15] B. C. Sales, B. C. Chakoumakos, D. Mandrus, J. W. Sharp, N. R. Dilley, and M. B. Maple, in *Thermoelectric Materials—The Next Generation Materials for Small-Scale Refrigeration and Power Generation Applications* (Ref. 6), p. 13.

[16] J. E. Graebner, B. Golding, and L. C. Allen, Phys. Rev. B **34**, 5696 (1986).